IJST, Transactions of Electrical Engineering, Vol. 35, No. E1, pp 25-43
Printed in The Islamic Republic of Iran, 2011

A NEW STRUCTURE FOR CURRENT-MODE CONTINUOUS TIME GM-C FILTERS*

S. J. AZHARI** AND M. SHOKOUFI

Faculty of Electrical Engineering, Iran University of Science and Technology (IUST),
Narmak, Tehran, I.R. of Iran, 1684613114
Email: azhari@iust.ac.ir

Abstract– In this paper a new structure for the MLF (Multi Loop Feedback) Gm-C group of filters is presented, granting the advantages of both current-mode and fully balanced topologies to the conventional structure of the group.

The ability of the structure to perform even more transfer functions (Low pass and Band Pass) than other members of the group is proved. Methods of enabling the proposed structure to perform other popular transfer functions are also presented. The favorite feature of systematical generation of the structure facilitates its arrangement for any order.

For practical comparison, a Butterworth 4^{th}–order LP filter with a cut-off frequency of 10MHz is designed in three different structures viz; the proposed one, the single-ended current mode, and fully balanced voltage mode. Simulation results show that the PSRR+,PSRR-,CMRR, Noise, THD, DR, consumed power (P) and Figure of Merit (FOM) of the new structure compared to its voltage mode counterpart are improved at least by factors of 36643, 59841, 4.75, 76, 2, 2.45, 1.17 and 509500, respectively. Compared to single ended current-mode type they are improved by factors of 40, 73, not defined, 1.3, 7.8, 150, 0.68 and 1763000, respectively. Although the above mentioned comparison, due to both the similarity of the used technology and the completeness of the results, is the most equitable one for the most definite conclusion, to further widen the extent of the comparison, the proposed structure is also compared with some other works yet assumed as its closet counterparts. This latter comparison also proves the certain superiorities of the proposed structure such that its FOM is from 8500 to 4512740 times larger than those of others. Closer tracking of the input signal at pass-band and more attenuation at stop-band are also achieved by this structure. These results strongly support the theoretical suggestions. Most favorably the much higher PSRR of the new structure makes it an extremely suitable choice for Mix-Mode (System-On- a Chip, SOC/SOI) applications where power supplies (and analog blocks) suffer severely from digital noise.

Keywords– Current-Mode filters, fully-balanced filters, very high FOM filters, very high PSRR/CMRR, very low THD filters, very low noise filters, very wide dynamic range filters

1. INTRODUCTION

In recent years a great deal of attention has been focused on Gm-C based filters, originating from such advantages as; high frequency operation, convenience of full integration, electronical tuning, calculation of components, and systematic generation of any order, a more flexible and simpler structure, and the smaller size of the topology, which matches well with the VLSI requirements [1-14].

There are many variants of Gm-C filters [1]-[14], among which the Multi loop Feedback (MLF) type has gained a distinguished place due to having all the advantages of the group. Moreover, it is less sensitive, more stable and capable of being configured with minimum components [4], [5], [7], [14]-[16]. It has been arranged in both voltage-mode and current-mode structures [1]-[5], [7], [14]-[16].

---

*Received by the editors September 3, 2009; Accepted May 30, 2011.
**Corresponding author

Due to the unique capabilities of current-mode structures, particularly in performing mathematical operations of filters' transfer functions [3]-[6],[9],[10], [12], [14],[15],[17]-[31], many current mode filters have been designed for which, compared to voltage mode counterparts, such advantages as wider bandwidth, broader dynamic range, lower THD, better inter modulation performance, and non-linear gain compression, multifunction canonic structure, smaller size, lower consumed power and lower power supply are reported [2]-[6],[9],[10],[12],[14],[15] and [17]-[31]. However, concerning MLF Gm-C filters, voltage mode types have more often been approached [4], [7], [11], [16] and [32].

Since fully balanced topologies offer such advantages as high CMRR and PSRR, low THD and noise and high accuracy [2], [11], [16] and [31]-[36], voltage mode versions of MLF Gm-C filters have frequently been implemented in this topology [11], [16], [32] and [34], while it has not yet been arranged for current mode MLF Gm-C filters to the best of the authors' knowledge. Hence by doing so, if possible, a very desirable continuous-time filter which exploits the outstanding capabilities of both fully balanced and current mode structures will be available. Meanwhile, to date, few works are claimed as implementations of fully balance current-mode filters [13]-[15] and [20]-[23]. However, these claims raise the two following objections. 1) None of these works have reported the values of such differential parameters as CMRR and PSRR, leaving the readers with just a bare claim that has to be supported by strong sufficient proof to be convincing. As exceptional cases [22] has reported the value of CMRR only, and [13] has given values of CMRR and PSRR, but both works (like all others) are liable to second objections as follows, 2) Some of those works are of voltage-mode type [13], and none are of MLF type but [15], again, has not reported the values of CMRR and PSRR, besides it is very heavy, noisy and power consuming.

In this paper, the structural feasibility of the idea of "current mode MLF Gm-C filter" is first practiced. The general theory and formulation of the proposed structure as well as its systematic development for any transfer function of any order are then given. To practically confirm the theory, simulation results of an LP Butterworth filter implemented in this new structure are included. Since a type-to type, spec- to-spec comparison has rarely been attempted the filter is also designed in two other leading configurations of MLF Gm-C filters viz, fully balanced voltage-mode (FBVM) and single ended current-mode (SCM). Their most important parameters are then compared.

2. FEASIBILITY STUDY OF THE IDEA

a) General structure

The structure shown in Fig. 1 seems to be a good candidate to implement the proposed idea;

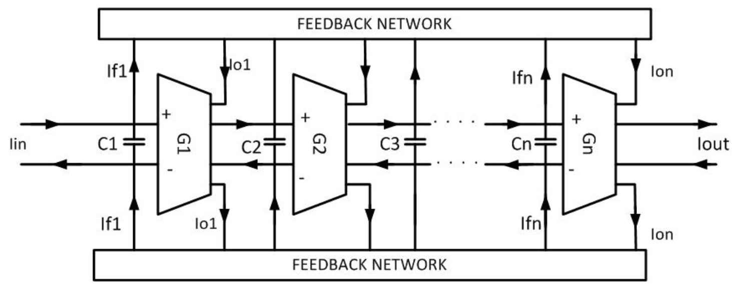

Fig. 1. Proposed implementation of the idea

It consists of a fully balanced multi loop current feedback network which can be arranged canonical with any number of loops depending on the demanded functions. Current feedback network provides low impedance nodes which enhance the frequency response of the topology. It also reduces the nodes' voltages causing the filter to work with lower supplies. Input-output signals of each stage in the feed forward path (Gm-C integrators) are also of current type, providing a fully current-mode processing discipline for the filter.

Figure 1 shows that not only the feedback network of the filter, but also feed forward section and all Gm-Cs are organized in fully balanced architectures supplying another necessity of the idea. To make this possible, as well as to properly perform the current feedback process (sampling output current- mixing input current) gm-amplifiers with at least four output terminals are used [25],[27]and [32]. For implementing band pass transfer functions two more output terminals are required, as is explained in section 3. It is worth noting that multi-output gm-amplifiers (used in this structure) are favored over the multi-input types which are utilized in voltage mode structure since the former types have a simpler circuitry and consume less power [11], [16], [32] and [34].

Figure 1 also shows that the structure balance is increased and the number of its components reduced by using floating capacitors, but at the expense of employing more costly technologies. Otherwise each floating capacitor can be replaced by two separate grounded ones, each of which is doubled in capacitance and connected to a separate node. The case, however, may increase the probability of the structure imbalance.

It can therefore be concluded that structural implementation of a fully balanced current-mode MLF Gm-C filter is generally feasible. To implement a more detailed structure we need to first investigate the theoretical feasibility as well as the formulation validity of the issue.

b) Theory and formulation

To study the theoretical operation of the proposed structure we develop the relation of its transfer function, H(s), for which by definition we have:

$$H(s)=\frac{I_{out}}{I_{in}}=\frac{I_{on}}{I_{in}} \tag{1}$$

While in Fig. 1 for the output stage we can write:

$$I_{On}=I_{out}=g_{mn}\times\frac{1}{C_nS}(I_{O(n-1)}-I_{fn}) \tag{2}$$

In (2), showing C_n/g_{mn} as τ_n gives:

$$S\tau_n I_{out}-I_{O(n-1)}=-I_{fn} \tag{3}$$

Similarly, for other stages we have:

$$\begin{gathered} S\tau_{n-1}I_{O(n-1)}-I_{O(n-2)}=-I_{f(n-1)} \\ S\tau_1 I_{O1}-(I_{O0}=I_{in})=-I_{f1} \end{gathered} \tag{4}$$

Combining all terms in (3) and (4) gives matrix (5):

$$[M(s)]\times[I_O]=[B]I_{in}-[I_f] \tag{5}$$

Where $[B]=[1\ \ 0\ \ \dots\ \ 0]^t$ and $$M(s)=\begin{bmatrix} S\tau_1 & . & . & . & \\ -1 & S\tau_2 & . & . & \\ & . & . & . & \\ & . & . & -1 & S\tau_n \end{bmatrix}$$

In this structure we arranged a canonic feedback network built by only short circuit connections between arbitrary outputs and inputs so that we have:

$$\left[I_f\right]=[F][I_0],\ \left[I_f\right]=\left[I_{f1}\ \ I_{f2}\ \dots I_{fi}\ \dots I_{fn}\right]^t\ ,\ \left[I_0\right]=\left[I_{01}\ \ I_{02}\ \dots\ I_{0i}\ \dots\ I_{0n}\right]^t \tag{6}$$

In (6) $[I_0],[I_f]and[F]$ are matrices presenting output currents of integrators, input currents of feedback networks and feedback factors relating each I_f to the appropriate I_o (i.e. f_{ij} is the factor by which I_{fi} is related to I_{oj}; $I_{fi} \propto f_{ij}.I_{oj}$), respectively. Superscript (t) stands for transpose which is the type of matrices. They are all defined by (3) to (5).

Combining (6) into (5) with some manipulation gives;

$$[A(s)]\times[I_0]=[B]I_{in} \tag{7}$$

$$[A(s)]=[M(s)]+[F]=\begin{bmatrix} S\tau_1+f_{11} & f_{12} & . & . & f_{1n} \\ -1 & S\tau_2+f_{11} & . & . & f_{2n} \\ & . & . & . & . \\ & . & . & -1 & S\tau_n+f_{nn} \end{bmatrix} \tag{8}$$

Thus for $H(s)$ we have:

$$H(s)=\frac{I_{out}}{I_{in}}=\frac{Io_n}{I_{in}}=\frac{[B]}{[A(s)]}=\frac{1}{|A(s)|}=\frac{1}{E_n s^n+\dots+E_i s^i+\dots+E_1 S+E_0} \tag{9}$$

Equation (9) is an all pole function proving that the proposed structure behaves like an n-ordered low pass filter, thus it is theoretically feasible too.

3. IMPLEMENTATION OF OTHER FUNCTIONS

Since performing all filter functions requires structures with general (arbitrary finite zero) transfer functions [7], [16] as is shown in (10) rather than all-pole type (9), the proposed structure seems to be of limited application.

$$H(s)=\frac{D_n S^n+\dots+D_i S^{n-1}+\dots+D_1 S^m+D_0}{E_n S^n+\dots+E_i S^i+\dots+E_1 S+E_0} \tag{10}$$

Since the same limitation exists in such leading types of MLF Gm-C filters as voltage-mode and single ended current-mode, some methods have been devised to overcome the problem [7],[10], [11], [16].

Although the same methods work properly here as will be discussed later, favorably the proposed structure on its own can perform BP and finite zeros functions as follows.

a) Selectable I/O method

In this method, as is shown in Fig. 2, in an n-ordered filter, ideally "n" pair of terminals exist for input or/and output signals which can arbitrarily be selected depending on the required transfer function.
However taking the output signal from any stage rather than the conventional one (here Gn) requires a gm-amp with two more output terminals (6 terminals altogether) in that stage. In such a case (8) will be changed to (11).

$$\begin{bmatrix} S\tau_1 + f_{11} & f_{12} & . & . & f_{1n} \\ -1 & S\tau_2 + f_{22} & . & . & f_{2n} \\ & . & . & . & . \\ & . & . & -1 & S\tau_n + f_{nn} \end{bmatrix} \begin{bmatrix} I_{o1} \\ I_{o2} \\ . \\ I_{on} \end{bmatrix} = \begin{bmatrix} I_{in1} \\ I_{in2} \\ . \\ I_{inn} \end{bmatrix} \tag{11}$$

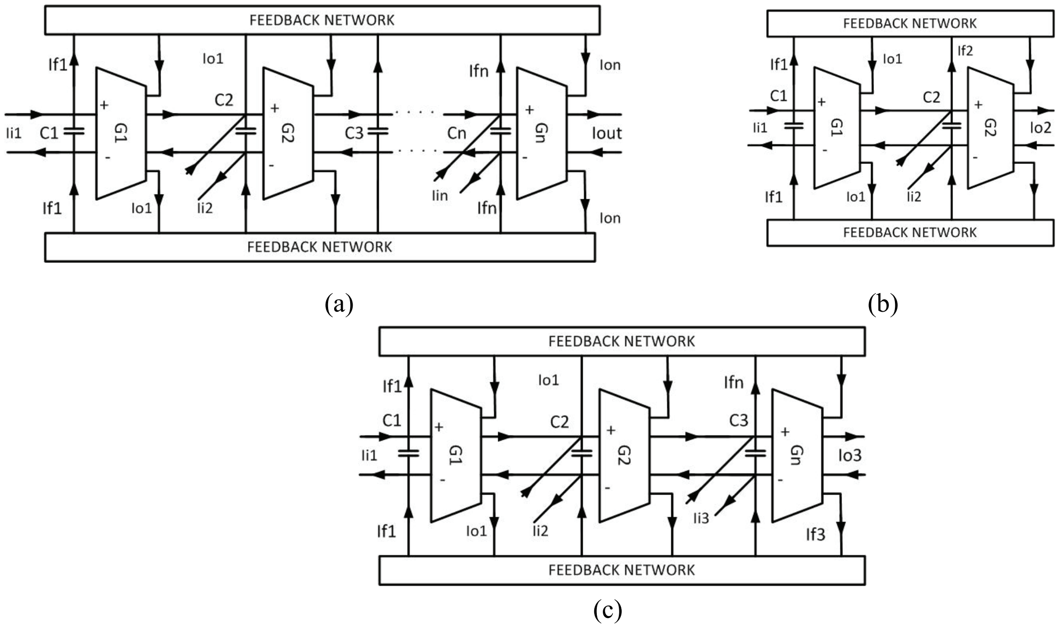

Fig. 2. Selected I/O implementation of the proposed idea (a): general structure (b): 2nd order filter (c): 3rd order filter

Although finding the general n-ordered transfer function of Fig. 2a is possible by solving (11) it is very tedious and time consuming, thus in this work as an example the equation is solved only for 2nd and 3rd order filters as follows.

1. Second order filter: A Second-order version of the proposed structure with two possible inputs and two possible outputs is shown in Fig. 2b. Solving (11) for n=2 obtains four different transfer functions, the formulation and the types of which are shown in (12) and Table 1.

$$\begin{bmatrix} I_{01} \\ I_{02} \end{bmatrix} = \frac{\begin{bmatrix} S\tau_2 + f_{22} & -f_{12} \\ 1 & S\tau_1 + f_{11} \end{bmatrix} \cdot \begin{bmatrix} I_{in1} \\ I_{in2} \end{bmatrix}}{(S\tau_1 + f_{11})(S\tau_2 + f_{22}) + f_{12}} \tag{12}$$

Table 1. Types of 2nd order filters realized by selected I/O method

I/O choice	I_{O1}	I_{O2}
I_{in1}	BP/LP	LP
I_{in2}	LP	BP/LP

Table 1 specifies that if, for example, the input signal is applied to the input port of the 2nd stage (I_{in2}) and the output signal is taken from the output port of the same stage, the proposed structure can behave like either a BP or LP filter depending on the parameters values of the transfer function of this particular choice, which is defined in (13).

$$\frac{I_{o_1}}{I_{in}} = \frac{S\tau_2 + f_{22}}{(S\tau_1 + f_{11})(S\tau_2 + f_{22}) + f_{12}} \tag{13}$$

2. Third order filter: The structure, formulations and types of the transfer functions of the 3rd-order selectable I/O version of the proposed structure are shown in Fig. 2c, Eq. (14) and Table 2, respectively.

$$\begin{bmatrix} I_{o1} \\ I_{o2} \\ I_{o3} \end{bmatrix} = \frac{1}{D} \times \begin{bmatrix} a_{11} & a_{12} & a_{13} \\ a_{21} & a_{22} & a_{23} \\ 1 & a_{32} & a_{33} \end{bmatrix} \begin{bmatrix} I_{in1} \\ I_{in2} \\ I_{in3} \end{bmatrix}$$
$$\begin{aligned} & a_{11} = (S\tau_2 + f_{22})(S\tau_3 + f_{33}) + f_{23}, \quad a_{12} = -f_{12}(S\tau_3 + f_{33}) + f_{13} \\ & a_{13} = f_{12} f_{23} - f_{13}(S\tau_2 + f_{22}), \quad a_{21} = (S\tau_3 + f_{33}) \\ & a_{22} = -f_{12}(S\tau_3 + f_{33}) + f_{13}, \quad a_{23} = -f_{23}(S\tau_1 + f_{11}) + f_{13} \\ & a_{32} = (S\tau_1 + f_{11}), \quad a_{33} = (S\tau_1 + f_{11})(S\tau_2 + f_{22}) + f_{12} \\ & D = (S\tau_1 + f_{11})(S\tau_2 + f_{22})(S\tau_3 + f_{33}) + f_{23}(S\tau_1 + f_{11}) + \\ & f_{12}(S\tau_3 + f_{33}) + f_{13} \end{aligned} \tag{14}$$

Table (2) shows that eight different types of BP and nine different types of LP filters can be realized by this structure.

Table 2. Types of 3rd order filters realized by selected I/O method

I/O choice	I_{O1}	I_{O2}	I_{O3}
I_{in1}	BP/LP	BP/LP	LP
I_{in2}	BP/LP	BP/LP	BP/LP
I_{in3}	BP/LP	BP/LP	BP/LP

These examples show that selectable I/O method does not need any further components and is preferred to those methods which add supplementary circuits to the basic structure. However, it cannot implement HP and BS functions for which other methods should be examined.

b) Supplementary circuits' methods

Two methods are reported to enhance the all-pole transfer function of fully-balanced voltage-mode and single-ended current-mode MLF Gm-C filters to arbitrary finite zeros type [7], [10] and [16]. They add two different supplementary circuits to the main structure. Although the final structure becomes more complex, massive, noisy and power consumptive than the selectable I/O type, it is capable of producing all filtering functions.

In this section we investigate the possibility of applying the same methods to the new structure as follows.

1. Input signal distributing method: In this method, in general, the input signal is concurrently applied to all nodes of the filter by a distributed network of G_m-amps, hence changing the overall transfer function. Examples of realized structures for fully balanced voltage mode and single ended current mode filters are given in [4], [16] and [10]. To apply the method to the new structure we designed a new distributing network compatible with a fully balance current-mode topology as is shown in Fig. 3a. To derive H(S) we follow the same procedure as obtaining (9), noting that here each node is also driven by distributed network, hence matrix [B] of (5) should be changed to:

$$[B] = \lfloor \alpha_1 \quad \alpha_2 \ \dots \ \alpha_j \ \dots \ \alpha_n \rfloor, \ \alpha_j = g_{dj} / g_r \tag{15}$$

While α_j, g_r and g_{dj} are the transmission factor of the input current of j^th integrator, gm parameters of input G_m-amp, and of j^th G_m-amp, respectively. Fig. 3a also shows:

$$I_{out} = \alpha_0 \, . \, I_{in} + I_{on} \, , \ \ \alpha_0 = g_{do} / g_r \tag{16}$$

It is thus concluded that:

$$H(S) = \frac{I_{out}}{I_{in}} = \frac{\alpha_0 |A(S)| + \sum_{j=1}^{n} \alpha_j A_{jn}(S)}{|A(S)|} \tag{17}$$

In (17) $A_{jn}(S)$ is j_n^{th} word of matrix [A(S)]. Equation (17) shows that the general structure and its developed version have the same poles determined by τ_i and f_{ij} coefficients, while the latter also includes transmission zeros arbitrarily produced by τ_i, f_{ij}, g_r and g_{dj}.

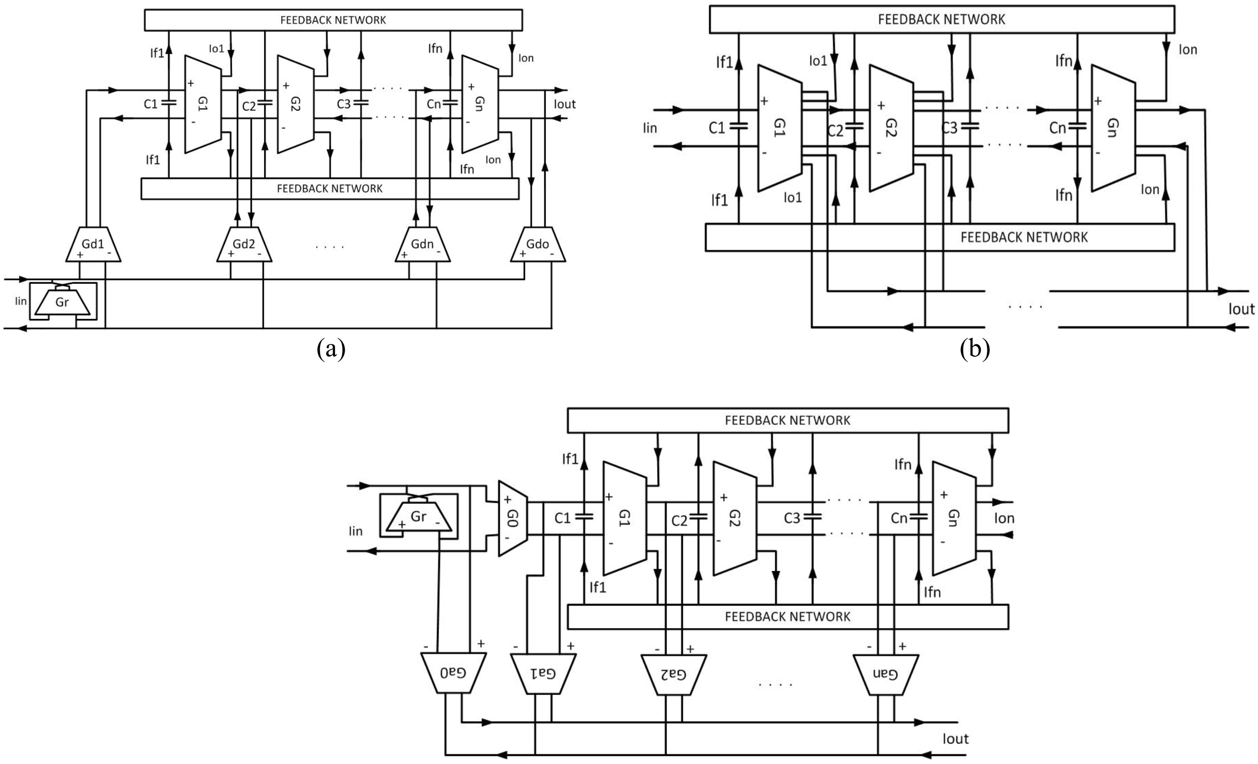

(a) (b)

(c)

Fig. 3. Realization of arbitrary finite zero filters by the proposed structure using methods of a) input current distribution b) direct summation c) indirect summation of output currents

2. Output signals summation method: In this approach a supplementary network is connected to the basic structure in such a way to provide an overall output as the sum of different nodes signal. Realization examples of the method for other configurations can be found in [4], [7], [10], and [16]. However two implementations of the method for the proposed structure are given in Figs. 3b and 3c. In Fig. 3b two more output terminals are provided for each G_m-amp except the last one (G_n). A summing network which is arranged by parallel connection of these terminals sums up the output currents of different stages forming the overall output current of the filter. Since both feedback and feed forward networks remain intact, the basic structure maintains the poles and the summing network forms the transmission zeros of the structure. Transmission coefficients can be determined by arbitrarily connecting or disconnecting the respective pair of new terminals. The magnitude of coefficients can be obtained by the aspect ratios (W/L) of the current mirror transistors responsible for new terminals. A negative sign when required is provided by interchanging the related connections. The problem with this realization is inflexible. That is, neither transmission coefficients nor design possible errors can be adjusted after fabrication. However it offers the advantages of simplicity, small size, less consumed power and less noise.

The flexibility merit can be gained by using the circuit shown in Fig. 3c in which a summation network is arranged by a set of G_m-amps shown as G_{ao}-G_{an} and input current is no longer applied directly, but through a new gm-amp (G_r) to both the input G_m-amp of the feed forward network (G_0) and the first gm-amp (G_{a0}) of the summation network. As a result g_m coefficients of G_m-amps of the summation network can be automatically or manually adjusted to zero or nonzero values for different applications. Summation network can also be wired up (connecting, disconnecting, interchanging) externally according to the required transmission zeros. The problems with this approach compared to the former are: circuit complexity, larger size, more consumed power and more noise. So one may choose either upon the circumstances. To find H(S), considering Fig. 3c we have matrix [B] of (5) as:

$$[B]=[r\ o \ldots o]^t \quad , \qquad r=\frac{g_0}{g_r} \tag{18}$$

Also, for I_{out} we have:

$$I_{out}=B_0\times r\times I_{in}+\sum_{J=1}^{n}B_J I_{OJ}\ ,\ B_j=\frac{g_{aj}}{g_j},B_0=\frac{g_{ao}}{g_o} \tag{19}$$

In which g_{ao}-g_{aj} and g_o-g_j are mutual transconductance of the G_m-amps of the summation and feed forward network, respectively. Referring to (6) - (8), (18) and (19) I_{oJ} can be obtained by (20) in which $A_{1j}(s)$ is the 1J[th] word of matrix [A(s)]:

$$I_{oj}=r\frac{A_{1j}(s)}{|A(s)|}I_{in} \tag{20}$$

Now using (19) and (20) we can find H(S) of Fig. 3c as (21) whose type is exactly the same as of (10).

$$H(s)=\frac{I_{out}}{I_{in}}=r\times\frac{B_o\times|A(s)|+\sum_{j=1}^{n} B_J A_{1J}(s)}{|A(s)|} \tag{21}$$

Comparing (21), (17) and (9) shows that also here, the poles are produced by the general section of the proposed structure while the supplementary circuit is responsible for the arbitrary finite transmission zeros.

4. SIMULATION RESULTS AND DISCUSSION

To practically investigate the performance of the new structure, a 4^{th} order Butterworth LP filter is designed. Based on what is explained in [9] and [16] ten different structures shown in Fig. 4 are also possible for canonical MLF fully balanced current mode 4^{th} order LP filter.

All of the G_m-amps of the filter are configured as is shown in Fig. 5 with transistors aspect ratios shown in Table 3. G_m-amplifier is designed so that when biased by ±3V power supplies, providing bias currents of 45µA for differential amplifier (M_1-M_2) and bias currents of 225µA for output current mirrors (M_5-M_8, M_{11}-M_{18}), and its gm-value is calculated as 185µS.

Table 3. Aspect ratios of MOSFETs that are used in the G_m-amp

Transistor	(W/L)
M_1, M_2	1/5
$M_3, M_4, M_6, M_8, M_{12}, M_{13}, M_{15}, M_{18}$	2/2
$M_5, M_7, M_{11}, M_{14}, M_{16}, M_{17}$	5/1
M_9, M_{10}	88/2

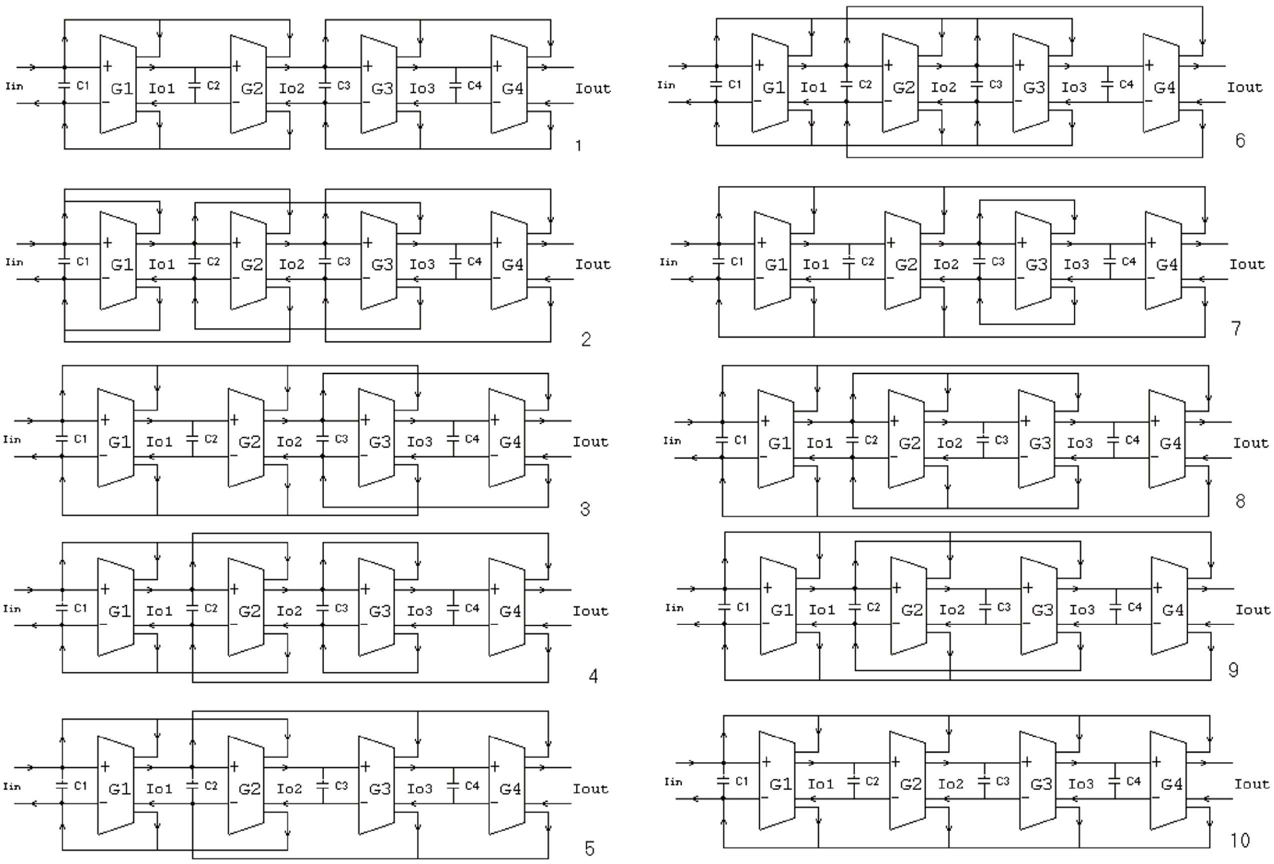

Fig. 4. Canonical fully balanced current mode structures of 4th order Butterworth low pass filters

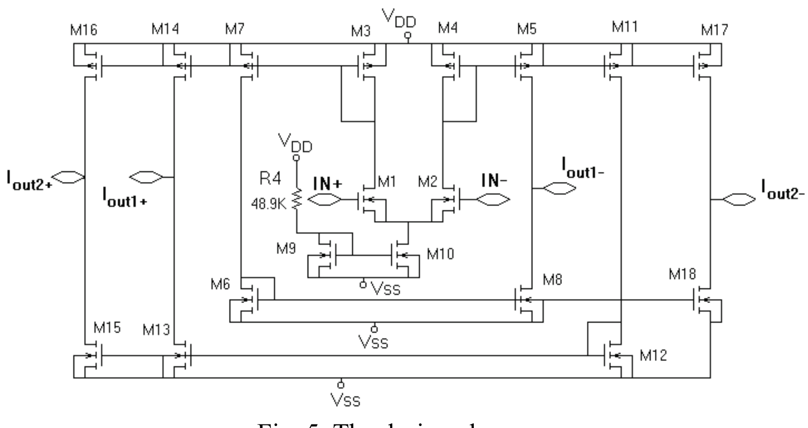

Fig. 5. The designed g_m-amp

The simulation values of the most important parameters of the designed G_m-amp when simulated with ORCAD (9.1) using HP 0.5μm CMOS N-well (CMOS14TB) parameters [37] are presented in Table. 4. For a filter cut-off frequency of 10MHz , g_m value of 185μS, time constants as are calculated in [31] and by using (2), values of floating capacitors of C_1-C_4 for all ten structures of Fig. 4 are calculated as presented in Table 5. In Fig. 6 simulated frequency response of all ten possible structures are compared with the response of an ideal filter of the same type labeled as (G_4), showing the closest-to-ideal response for structure no.2 in Fig. 4, thus henceforth it is chosen for investigation.

Table 4. Simulation results of the used Gm-amp

Specification	Simulation results
Supply voltage	±3V
Cut- off frequency	175.751MHz
THD	1.1 %@3Vp-p,500KHz
gm	185µs
PSRR+	58.4db
PSRR-	34.8db
CMRR	82db
Noise	Till 175.75Mhz 7.62 $pA/\sqrt{Hz}$
	Total at filter pass band 24.1nA$_{rms}$
Power dissipation	6.6mW

Table 5. Capacitors' values calculated for proposed structures of Fig. 4 while begin used to implement the given 4th order Butterworth filter

	C_4	C_3	C_2	C_1
1	2.25352pF	3.846997 pF	5.44048 pF	1.593494 pF
1	5.44048 pF	1.593474 pF	2.253521 pF	3.84699 pF
2	4.50703 pF	4.643738 pF	3.186953 pF	1.126759 pF
3	5.02455 pF	5.48069 pF	2.489438 pF	1.126759 pF
4	5.727676 pF	2.638962 pF	2.52872 pF	1.96632 pF
5	6.567232 pF	3.38028 pF	3.0047 pF	1.126759 pF
6	6.567232 pF	4.5070 pF	2.25352 pF	1.126759 pF
7	7.6940 pF	1.964976 pF	1.88202 pF	2.64139 pF
8	7.6940 pF	1.88202P	2.64139 pF	1.96407 pF
9	7.6940 pF	2.72024 pF	3.18695 pF	1.126759 pF
10	7.6940 pF	3.84699 pF	2.25352 pF	1.126759 pF

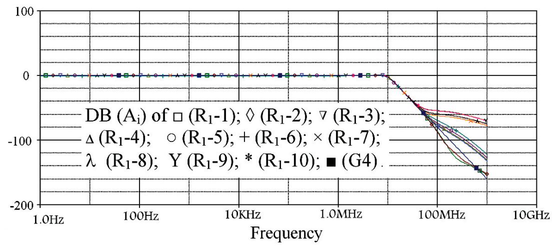

Fig. 6. Comparison of frequency responses of filters which are shown in Fig. 4 (R1-1 to R1-10) with an ideal response (G4)

THD behavior as well as simulated values of the most important specification of this structure operating at ±3V supplies are shown in Fig. 7 and Table 6.

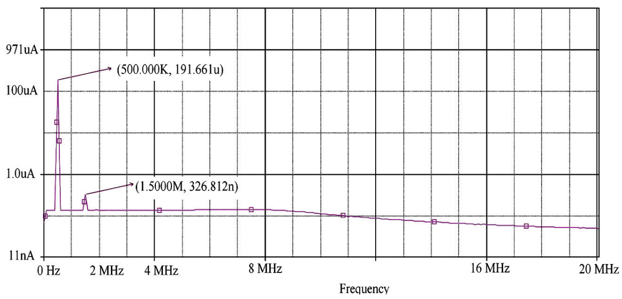

Fig. 7. THD performance of the simulated 4th order fully balanced current mode low pass filter

Figure 7 shows the great advantage of the new structure in rejecting even harmonics and reducing odd ones producing a THD of 0.18% (-55db) while driven by an input current signal with frequency of

500KHz and a p-p amplitude of 400μA (9 times larger than the bias current of dif. Amp., M_1-M_2). This shows a nearly 6 fold improvement compared to g_m-amp THD, thanks to fully balance scheme which also significantly improved the PSRR, CMRR and DR of the filter. Using conventional definition for current mode case [38] CMRR, PSRR+, and PSRR- were measured as infinite (here 600db due to the predetermined resolution default of the simulation software) for the ideal transistors of the filter.

Table 6. Simulation results of the given 4th order fully balanced current mode LP filter at $Vs = \pm 3volts$

Specification	Simulation results	
AI	0.978	
THD	0.18%@400μAp-p,500KHz	
CMRR	Ideal	600db
	MC(WC)*	50.5db
PSRR+	Ideal	600db
	MC(WC)*	136.64db
PSRR-	Ideal	600db
	MC(WC)*	136.64db
Noise	4.5 pA/$\sqrt{Hz}$ till 1MHz	
	36 nA_{rms} total noise at passband	
D.R(THD=0.18%@I_{in}=400μA_{pp})	143.77db	
Cut off frequency	10.4MHz	
Power dissipation	45.3mW	
*Monte Carlo (Worst case) simulation for 10% V_t mismatches		

To get a realistic understanding, Monte Carlo analysis allowing 10% mismatches for V_t of the transistors was executed showing the worst case values as 50.5 db, 136.64db, 136.64db for CMRR, PSRR+, PSRR-, respectively (Table 6 and Fig. 8).

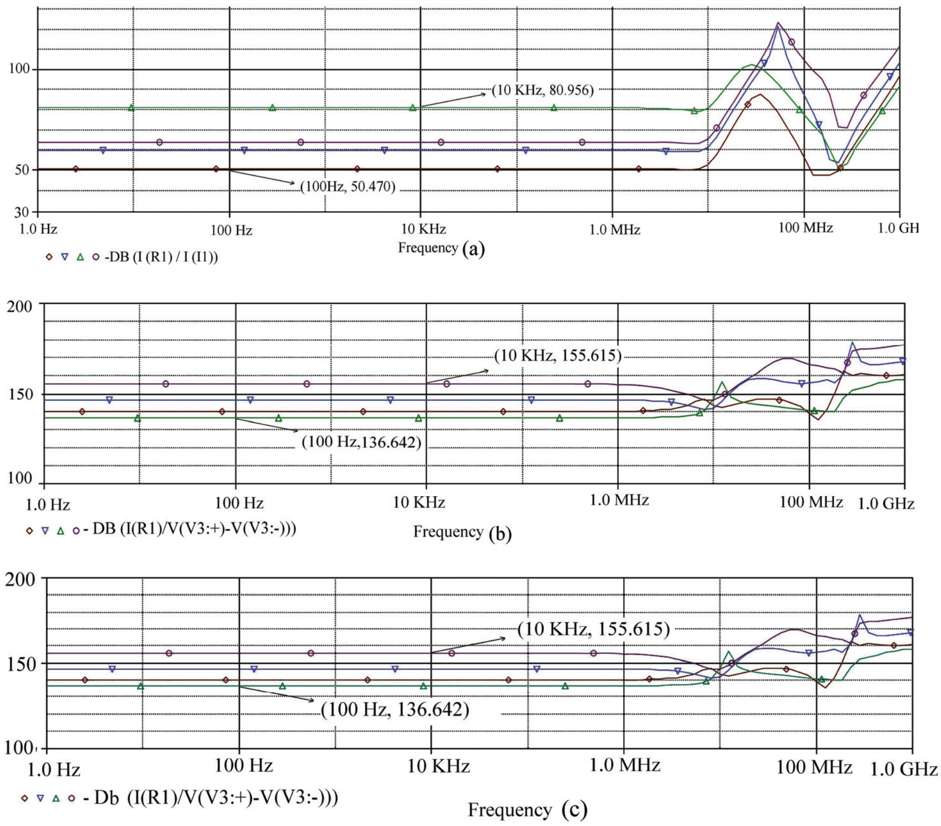

Fig. 8. Monte Carlo analysis of the fully balanced current mode filter with 10% variation of Vt
(The ideal pass is not shown) a) CMRR, b) PSRR+, c) PSRR

To calculate DR, the definition shown as (22) is adopted [28], taking the values of the parameters from Table 6 and Fig. 12.

The very high value of 143.8db is calculated for DR of the proposed structure at THD of 0.18%, which is basically due to both the low value of THD and the noise of the fully-balance scheme. To compare, the same filtering function is implemented and examined in two other favorite structures of the group as follows.

$$DR = \frac{(signal_{rms})^2 \, @ \, a\%THD}{(noise)^2} \tag{22}$$

a) Single-ended current mode (SCM) structure

This structure is a well known frequently used one whose 4th-order LP version can be configured in ten different forms [8]. They are realized and their frequency responses for Butterworth LP function with 10MHz cut-off frequency are shown in Fig. 9 [31]. It is worth noting that in this structure gm-amps need only two output terminals resulting in a smaller size than that of the current work (Figs. 4-5).

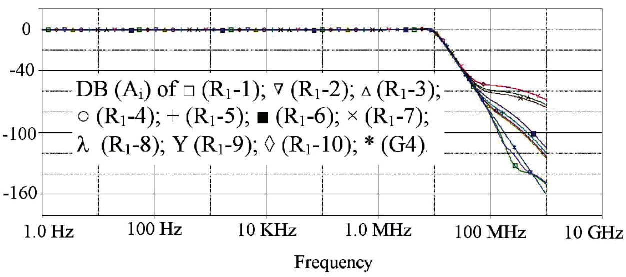

Fig. 9. Frequency responses of all possible structures of single-ended current mode version of the filter of instance

Both theory [4], [7], [8] and simulation (Fig. 9) show that the structure of Fig. 10 (labeled as R_{1-2} in Fig. 9) is the closest- to-ideal one (G_4 in Fig. 9) and thus, is chosen for comparison. The values shown in Figs. 11-13 and Table 7 are found for the SCM structure at the same conditions as of Table 6.

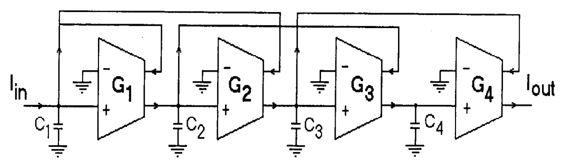

Fig. 10. Single-ended current mode structure chosen for comparison

Comparing Figs. 7 and 11 obviates that the new structure provides a THD which is 7.8 times less than that of the SCM structure. Therefore, to sustain identical THD for both structures the amplitude of the input current of the SCM is decreased to 40µAp-p(0.1of that of new structure). This point along with the rather better noise performance of the new structure (Fig. 12) results in a DR value for the SCM which is 150 times less than that of the new structure (Tables 6 and7). The ideal values of PSRR+ and PSRR- of the SCM structure is about 490db less than that of the new structure, while their Monte Carlo Worst Case values are less, about 35-40db (Cf. Fig. 13 and 8). Although their behavior outside the pass band is of much less importance, it is even worse in this area, reflecting the much better performance of the new structure at higher frequencies (Fig. 8). On the contrary, the power consumption of SCM is quite less (2/3) than that of the new structure due to the smaller size of the former one (Tables 6-7).

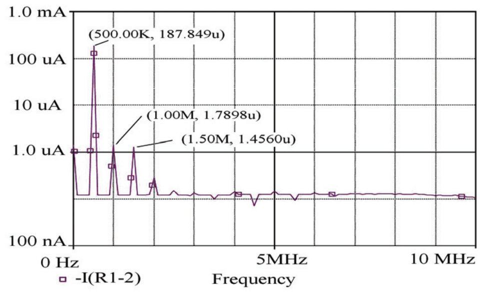

Fig. 11. THD response of the filter shown in Fig. 10

Table 7. Simulation results of the unbalanced current mode version of the given filter at $Vs = \pm 3volts$

Specification	Simulation results	
AI	0.942	
THD	1.32%@400μA$_{p-p}$,500KHz	
PSRR+	Ideal	111.6db
	MC(WC)*	104.5db
PSRR-	Ideal	108.7db
	MC(WC)*	99.4db
Noise	8.9 pA/ $\sqrt{Hz}$ till 1MHz	
	44.24 nA rms total noise at pass band	
DR @ (THD = 0.18%@Iin=400μApp)	100.2db	
Cut off frequency	10.95MHz	
Power dissipation	30.4mW	
*Monte Carlo (Worst case) simulation for 10% V_t mismatches		

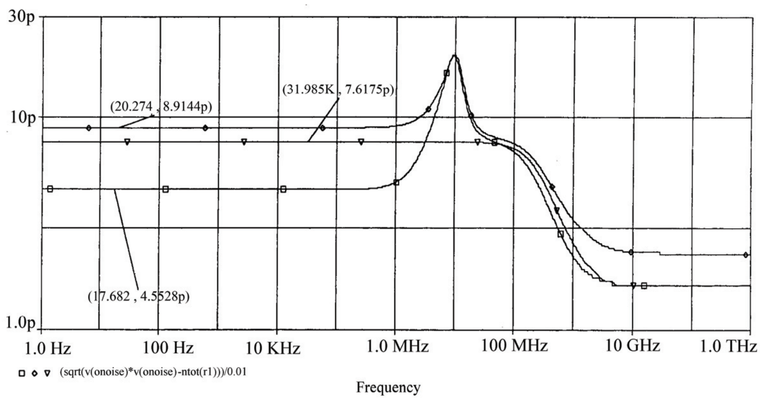

Fig. 12. Noise comparison between new structure (□), single ended type (◊) and OTA (∇)

b) Fully balanced voltage-mode (FBVM) structure

As is expressed in [7] this structure can also appear in ten different versions, while being used to implement a 4th-order MLF canonical Butterworth LP filter. Among these versions the one in Fig. 14 shows the best performance and so is used for comparison.

To build the special gm-amps (with 4 input and 2 output terminals and Gm=185μS) of the structure two of the Gm-amps used in the SCM version (Fig. 10) are combined with their output terminals connected in parallel.

With filter cut-off frequency of 10 MHz, the following values are calculated for the capacitors [7], [31];

$$C_1=4.50703pF,\ C2=4.654738pF,\quad C_3=3.186953pF,\quad C_4= 1.126759pF$$

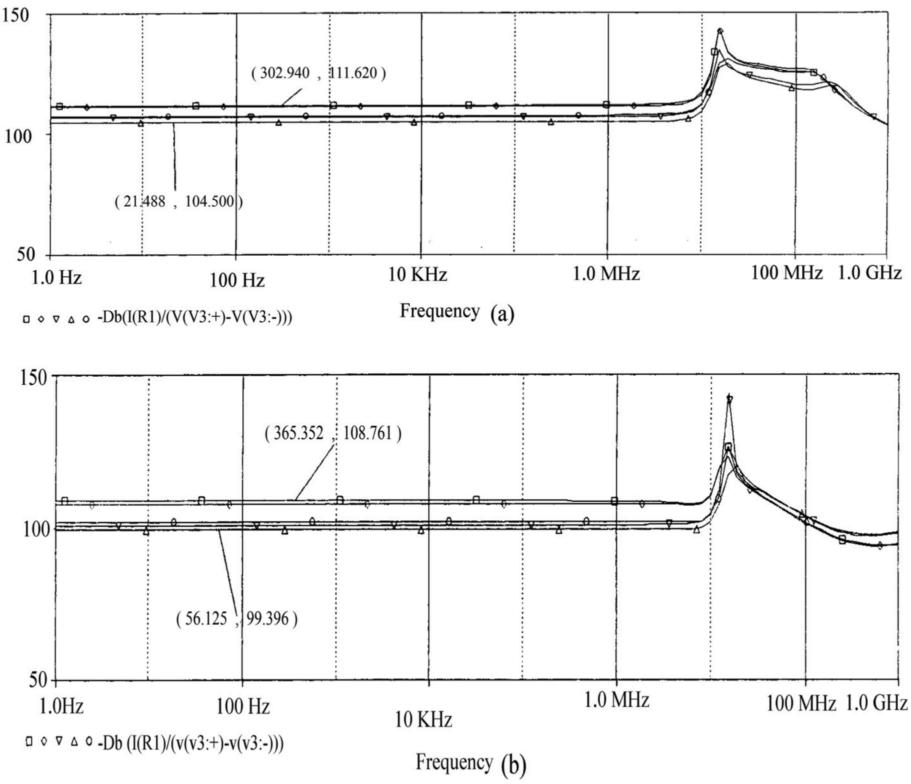

Fig. 13. Monte Carlo analysis of single-ended structure (Fig. 10) in the same condition as of Fig. (8), a) PSRR+, b) PSRR- (ideal pass is not included)

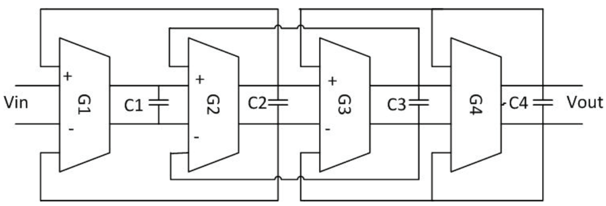

Fig. 14. Fully balanced voltage mode counterpart of the new structure

Frequency response simulation of this structure compared with the ideal response of the type is shown in Fig. 15 and the simulation results of its most important parameters are shown in Table 8 and Figs. 16-18.

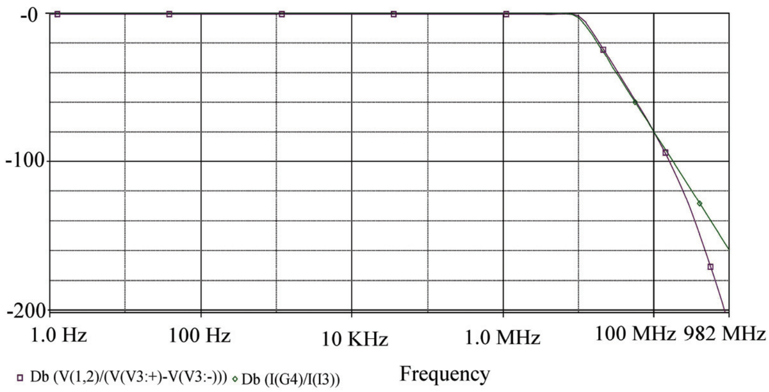

Fig. 15. Simulated frequency response of; □) the filter shown in Fig. 14 compared with ◊) the ideal response

Table 8. Simulation results of the fully balanced voltage mode version of the given filter at Vs=±3V

Specification	Simulation results	
Av	0.9601	
THD	0.42%@2.85V_{p-p},500KHz	
CMRR	Ideal	600db
	MC(WC)*	36.96db
PSRR+	Ideal	600db
	MC(WC)*	45.36db
PSRR-	Ideal	600db
	MC(WC)*	41.1db
Noise	74.7 nV/$\sqrt{Hz}$ till 1MHz	
	272µV_{rms} total noise at pass band	
Cut of frequency	10.868MHz	
D.R THD=0.18%@Vin=2.15Vpp)	137.7db	
Power dissipation	52.9mW	
*Monte Carlo (Worst case) simulation for 10% Vt mismatches		

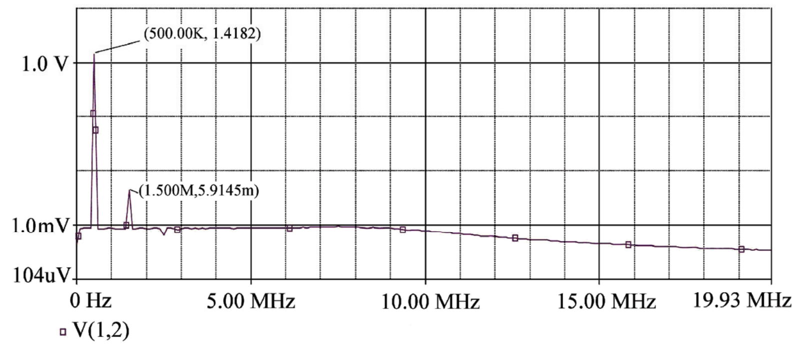

Fig. 16. THD response of the fully-balanced voltage mode filter of Fig. 14

As an important technological advantage, the components count of the new structure is about 2/3 that of the FBVM version which results in; integration easiness, chip size and cost reduction, as well as less power consumption (here 20%), however, this condition is reversed compared to the SCM structure. Better input tracking (gain of the filter) at pass band and more attenuation at stop band (cf. Figs. 6, 9 and15) are other merits of the new structure

The most important parameters in comparing filters efficiency is believed to be; Power Dissipation (P), (characteristic) Frequency (Fo), Tuning Range (Δf), and Dynamic Range (or S/N at a specified level of THD), while CMRR and PSRR are especially important in mixed-mode chips. To encapsulate all these factors a parameter called Figure Of Merit (FOM) is defined [20], [24]. This is very usual in analog continuous time circuits, contrary to digital circuits that work based on discontinuous time signals [25].In this work, since (Fo) is intentionally set fixed and equal for all three structures, we have expressed FOM as:

$$FOM = \frac{(DR\ @\ 0.18\%THD) \times PSRR \times CMRR}{P} \tag{23}$$

In (23) the PSRR is the average value of PSRR+ and PSRR- which are very important parameters in mixed-mode where filters are integrated on the same chip with digital circuits.

In Table 9 the most important parameters of the new structure and those of two other implemented ones (in this work) are compared with the reported parameters of some other close works. Other works are included just to further widen the extent of comparison, while only one of which (in addition to those three types simulated in this work) is claimed by the authors (and implies the structure) to be MLF and the rest are (at least) differential Gm-C (mostly CM) types. For further reliable results, either fabricated structures or those with Monte Carlo simulation results are chosen (with the exception of [15], the only CM. FB. MLF one and [21]). Since the reported results of other works (with the exception of current work) are neither complete nor belong to the same parameters, for a fair comprehensive comparison, four FOMs other than (23) are defined as follows:

$$\mathrm{FOM1} = \frac{CMRR \times PSRR \times F_0}{THD \times P} \quad , \quad \mathrm{FOM2} = \frac{CMRR \times F_0}{THD \times P} \tag{24}$$

$$\mathrm{FOM3} = \frac{F_0 \times N \times DR}{P} \quad , \quad \mathrm{FOM4} = \frac{F_0 \times N}{THD \times Noise \times P}$$

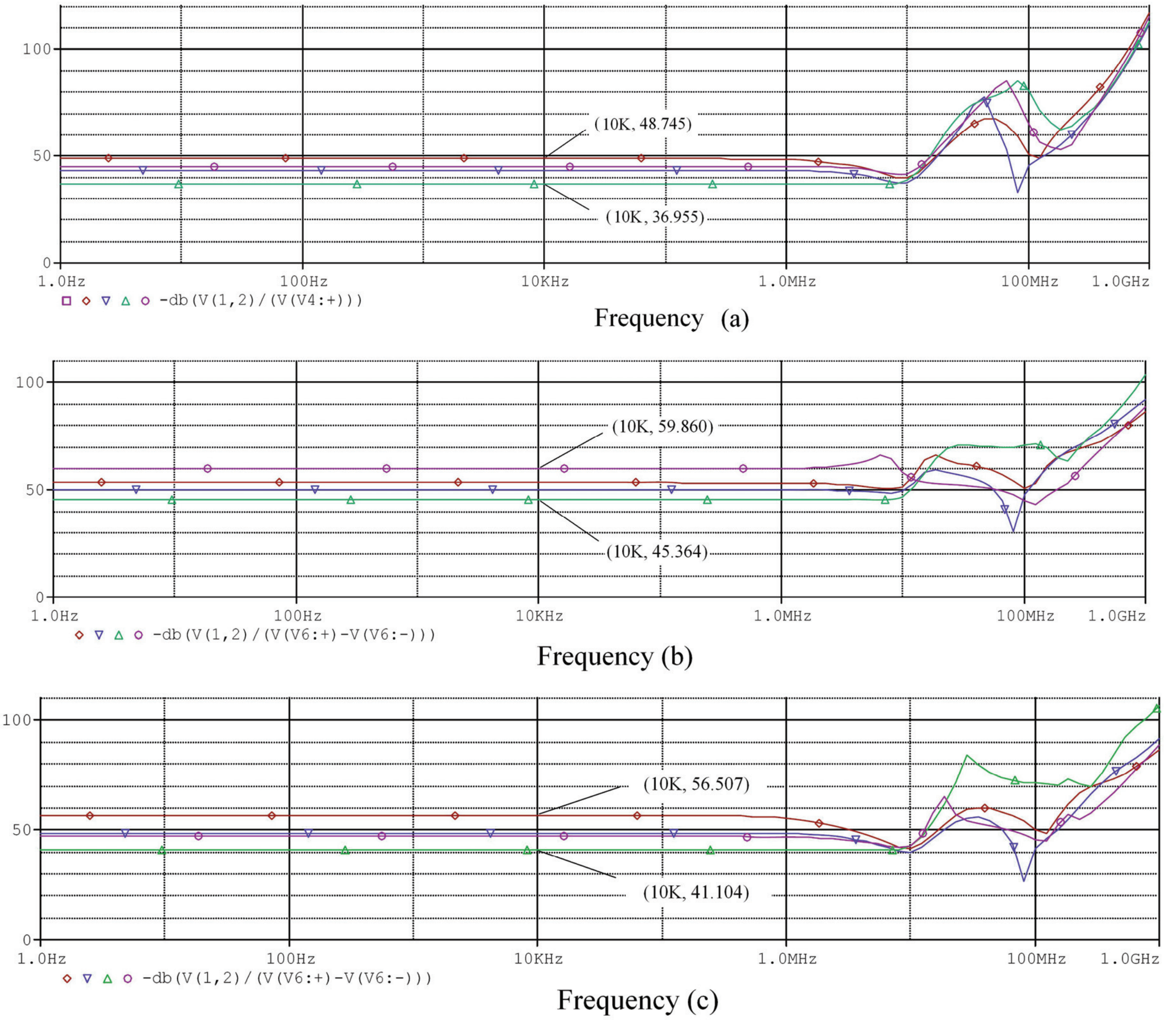

Fig. 17. Monte Carlo analysis of fully-balanced voltage mode structure in the same conditions as of Fig. 8, a) CMRR, b) PSRR+, c) PSRR-

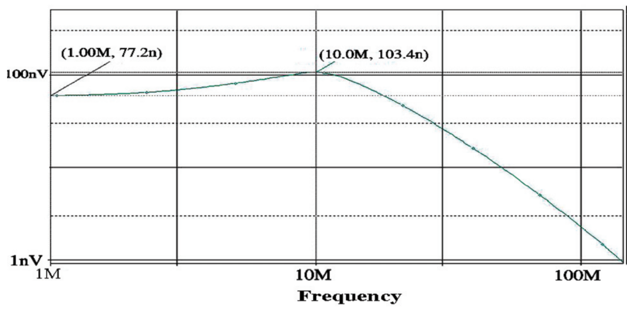

Fig. 18. Noise response of fully-balanced voltage mode structure

They are used to evaluate the overall performance of [13], [21], [15 and20], and [22] while current work structures are evaluated by FOM of (23) and FOM4, since the latter is the only one which includes the value of noise. The table shows that FOM of the new structure is 1763000 times and 509500 times better than those of single-ended Current-Mode and Fully-Balanced Voltage-Mode structures, respectively. It is from 8500 to 451274 0 times larger than other works (3456100 times larger than another MLF one reported by other authors [15]).It also shows that, the new structure has integrated the fully-balanced scheme advantages such as; less THD, larger CMRR, PSRR and DR with the current-mode superiorities resulting in much larger improvement for those advantages which are in common in both fully balanced and current mode schemes.

Table 9. Comparing important parameters of single-ended current mode and fully balanced voltage mode filter and some other close works with those of proposed structure.

Ref. No.	[13]	[15]	[20]	[21]	[22]	CM, Single ended (This work)	VM, FB (This work)	CM , FB This work (Proposed)
Filter type	3rd order VM,FB, Chebyshev	5th order, CM,FB, MLF	3rd order, CM, Dif. Butterworth	3rd order, CM Dif. wave Active	13th order, CM, dif. wave active	4th order CM-MLF	4th order FB-VM-MLF	4th order FB-CM-MLF
Technology	Fabricated in 0.18μm	0.18μm	Fabricated 65nm	0.35μm	Fabricated 0.35μm	0.5μm (MC)[1]	0.5μm (MC)[1]	0.5μm (MC)[1]
F0	150K~ 23MHz	28M~44MHz	1M~4MHz	1M~10MHz	4.1MHz	10.95MHz	10.868MHz	10.4MHz
CMRR	-37db	NA	NA	-90db~ -50db	NA	NA	36.96db	50.5db
PSRR	-35db	NA	NA	NA	NA	104.5db	45.36db	136.64db
THD	0.25% -0.63% @ Vin=100mV	1% @10MHz @Iin=600μA	1%@277μA@ 100KHz	1.78%@Iin= 64μA	0.5%@500K Hz	1.32%@400μA p-p500KHz	0.42%@2.85 Vp-p,500KHz	0.18%@400μ Ap-p,500KHz
DR	NA	62-67db	74db~68db @Vin=0.5V	NA	NA	100.2db	137.7db	143.77db
Vsup	NA	NA	1V	±2.5	±2.5	±3	±3	±3
Power	18mW	67mW@30M Hz	9.6mW	14.8mW	178mW	30.4mW	52.9mW	45.3mW
Noise	NA	270nV/$\sqrt{Hz}$	40pA/$\sqrt{Hz}$	NA	125dbm/H 17.8n/$\sqrt{Hz}$	8.9pA/$\sqrt{Hz}$	74.7nV/$\sqrt{Hz}$	4.5pA/$\sqrt{Hz}$
FOM	----------	------------	-----------	-----------	---------	4.396×10^{11} (FOM)	1.52×10^{12} (FOM)	7.75×10^{17} (FOM)
	8.07×10^{14} (FOM1)	4.1×10^{12} (FOM3)	3.14×10^{12} (FOM3)	1.2×10^{13} (FOM2)	1.66×10^{15} (FOM4)	2.467×10^{18} (FOM4)	7.19×10^{14} (FOM4)	1.417×10^{19} (FOM4)

1) - MC = Monte Carlo Simulation is performed to get the results

5. CONCLUSION

In this work the fully-balanced current mode version of continuous-time MLF Gm-C filters is successfully implemented. The theory of its operation is thoroughly developed and precisely formulated. The block in its simplest form performs an all-pole transfer function. It can also perform BP functions using selectable I/O method. The claim has been proved by examples. Besides, by some minor modification it gained the capability of performing all conventional filtering functions using methods of input signal distributing, and output signal summation.

Structurally integrating the fully-balanced topology, current-mode discipline and MLF Gm-C scheme provided the new structure with such outstanding advantages as: extremely large PSRR, very large CMRR, very wide DR, extremely low noise, very low THD, extremely better FOM, low consumed power, low level power supplies, small size, systematical development to any order, better input signal tracking at pass band and more attenuation at stop band. To practically study the performance superiority of the new structure, a 4th-ordered Butterworth LP filter has been implemented by both the new structure and two other leading structures of MLF Gm-C filters; unbalanced current-mode and fully-balanced voltage-mode types. These three types are compared together and also with some other differential Gm-C filers (preferably current-mode MLF types although so far very few have been reported). The results are in good agreement with the theory and strongly support the superiorities of the proposed structure.

REFERENCES

1. Sanchez-Sinencio, E. & Silva-Martinez, J. (2000).CMOS transconductance amps architectures and active filters: A tutorial. *Proc. of IEEE Circuits Devices Syst*. Feb, Vol. 147, No.1: pp. 3-12.
2. Ananda Mohan, P.V. (2003). *Current-mode VLSI analog filters, design and application*. Birkhauser Boston,
3. Ahmad Rania, F., Awad Inas, A. & Soliman Ahmad, M. A. (2006). Transformation method from voltage-mode Op-Amp-RC circuits to current-mode Gm-C circuits. *Circuits Systems Signal Processing*, Vol. 25, No. 4, pp. 609-26.
4. Su, H. W. & Sun, Y. (2005). Performance analysis and comparison of multiple loop feedback OTA-C filters. *Journal of Circuits, Systems, and Computers*, Vol. 14, No. 4, pp. 1–36.
5. Deliyannis, T. L., Sun, Y. & Fidler, J. K. (1999). *Continuous-time active filter design*. CRC Press.
6. Qadir, A. & Altaf, T. (2010). Current mode canonic OTA-C universal filter with single input and multiple outputs. *2nd International Conference on Electronic Computer Technology (ICECT2010)*, pp. 32-34.
7. Sun, Y. & Fidler, J. K. (1997). Structure generation and design of MLF OTA-grounded capacitor filters. *IEEE Trans. On CAS-1*, Vol. 44, No.1, pp. 1-11.
8. Sun Y., Fidler J. K. (1995). Minimum component multiple integrator loop OTA-grounded capacitor all-pole filters *Proc. of IEEE Midwest Symp*. On CAS, USA. pp. 983-6
9. Sun Y., Fidler J. K. (1995).High-order current-mode continuous-time multiple output OTA-C filters. *IEE 15th Sarag. Colloq. Digital and Analogue Filters and Filtering Systems*, U.K.P. 8/1-6.
10. Sun Y., Fidler J. K. (1996). Current-mode OTA-C realization of arbitrary filter characteristics. *Electronics Letters*, Vol. 32, No. 13, pp. 1181-2.
11. Chiang, D. H. & Schumann, R. (1999). Comparison of magnitude and delay sensitivity in IFLF and cascade Gm-C filters. *IEEE Int. Symp. on CAS-II, ISCAS'99*, pp. 652-5.
12. Shaker, M. O., Mahmoud, S. A. & Soliman, A. M. (2006). A CMOS fifth-order low-pass current-mode filter sing a linear transconductor. *P1043-1046 Circuits and Systems*, 2006. ISCAS 2006.
13. Gao, Z., Wang, J., Lai, F., Yu, M. & Zhang, Z. Z. (2009). Wideband reconfigurable CMOS Gm-C filter for wireless Applications, Electronics, Circuits, and Systems, *ICECS 2009. 16th IEEE International Conference*, pp. 179-182
14. Hwang, Y. S., Chen, J. J., Laiand, J. H. & Sheu, P. W. (2006). Fully differential current-mode third-order Butterworth VHF Gm-C filter in 0.18 μm CMOS. *IEE Proc. Circuits Devices Syst.*, Vol. 153, No. 6, pp. 552-558.
15. Zhu, X., Sun, Y. & Moritz, J. (2008). Design of current-mode Gm-C MLF elliptic filters for wireless receivers, Electronics, Circuits and Systems, *ICECS 2008. 15th IEEE International Conference*, pp. 296-299.
16. Sun, Y. & Fidler, K. (1998). Fully-balanced structures of continuous-time MLF OTA-C filters. *IEEE Int. Conf. Circuits and Systems*, pp. 157-60.
17. Sun Y., Fidler J. K. (1997). Current-mode multiple feedback filters using dual output OTAs and grounded capacitors. *Int. J. of Circuit Theory and Applications*, Vol. 25, pp. 69-80,.
18. Dalibor BIOLEK1 Viera BIOLKOVA (2010). Current-input current-output 2nd-order all-pass filters employing two ZC-CITAs. *2010 20th International Conference Radioelektronika IEEE Conferences*, pp. 1-4.

19. Laoudias, C., & Psychalinos, C. (2008). Low-voltage CMOS current-mode filters using current mirrors: two alternative approaches. *Electrotechnical Conference, 2008. MELECON The 14th IEEE Mediterranean*, pp. 435-440.
20. Heimo, U. & Zimmermann, H. (2008). A1VCurrent-mode filter in 65nmCMOS using capacitance multiplication. *IEEE 2008 System-on-Chip, 2008. SOC 2008. International Symposium*, pp. 1-4
21. Souliotis, G. & Haritantis, I. (2005). Current-mode differential wave active filters. *IEEE Transactions On Circuits And Systems—I: REGULARPAPERS*, VOL. 52, NO. 1, pp. 93-98.
22. Souliotis, G. & Fragoulis, N. (2006). Differential current-mode tunable wave active filters based on single-ended wave port terminators. *IEEE Transactions on CAS—I*: Regular Papers, VOL. 53, No. 4, pp. 821-828.
23. Souliotis, G. & Psychalinos, C. (2008). Current-mode linear transformation filters using current mirrors. *IEEE Transactions on Circuits and Systems—II: Express Briefs*, Vol. 55, No. 6, JUNE2008, pp. 541-5.
24. Chamla, D., Andereas, K., Cathelin, A., Belot, D. (2005). A Gm-C low-pass filter for zero-IF mobile applications with a very wide tuning rang. *IEEE J. of SSC.* Vol. 40, pp. 1443-50
25. Shahrtash, S. M. & Haghjoo, F. (2009). Instantaneous wavelet transform decomposition filter for on-line applications. *Iranian Journal of Science & Technology, Transaction B: Engineering*, Vol. 33, No. B6, pp. 491-510.
26. Toumazou, C., et.al. (1990). *Analogue IC design: the current mode approach*. London, Peter Peregrinus,
27. Hsu, C. C. & Feng, W. S. (2000). Structural generation of CM filters using multiple-output OTA. *Trans. Fund. Electronic, Communication, Computer Science*, Vol. E 83-A, No. 9, pp. 1778-85.
28. Georgantas, T., Bouras, S., Dervenis, D. & Papananos, Y. (1999). A comparison between integrated current and voltage mode filters for baseband applications. *Proc. of 6th Int. Conf. of Electronics, Circuits and Systems*, pp. 485-8.
29. Zele, R. H., Allstot, D. J. & Fiez, T. S. (1993). Fully balanced CMOS current-mode circuits. *IEEE J. of Solid-State Circuits*, Vol. 28. No. 5, pp. 569-75.
30. Sun, Y. & Fidler, J. K. (1995). Structure generation of current-mode two integrator loop dual output-OTA grounded capacitor filters. *IEEE Trans. On CAS.- II*, Vol. 43, pp. 659-63.
31. Shokoufi, M. (2002). Design of a current-mode fully balanced Butterworth low pass Gm-C filter in CMOS technology. M. Sc Thesis, Iran University of Science and Technology (in Farsi).
32. Glinianowicz, J., Jakusz, J., Szczepanski, S. & Sun, Y. (2000). High-frequency two-input CMOS OTA for continuous-time filter applications, *IEE Proc. Circuits Devices Syst.*, Vol. 147, pp. 13-18.
33. Sansen W. N. C. (2006). Analogd Esign Essentials, Springer.
34. Wyszynski, A. & Schumann, R. (1992). Using multiple-I/P transconductors to reduce number of components in OTA-C filter design. *Electronic Lett.*, Vol. 28, pp. 217-20.
35. Vanpeteghem, CP. M. & Duque-Carrillo, J. F. (1990). A general description of common-mode feedback in fully-differential amp. *IEEE Int. symp. On CAS*, pp. 3209-12.
36. Saniei, N. & Djahanshahi, H. (2007). A high speed SiGe VCO based on self injection locking scheme. *Iranian Journal of Science & Technology, Transaction B: Engineering*, Vol. 31, No. B6, pp. 651-662.
37. Baker, R. J., Li, H. W. & Boyce, D. E. (1998). *CMOS circuits design, layout, and simulation*. IEEE Press.
38. Palmisano, G., Palumbo, G. & Pennisi, S. (1999). Performance parameters of COAs. *Proc. of IEEE, ICECS*, pp. 1615-18.